Synthetic and Systems Biotechnology 7 (2022) 815–823

Contents lists available at ScienceDirect

Synthetic and Systems Biotechnology

journal homepage: www.keaipublishing.com/en/journals/synthetic-and-systems-biotechnology

Original Research Article

Putative functions of EpsK in teichuronic acid synthesis and phosphate starvation in *Bacillus licheniformis*☆

Yiyuan Xu [a,b], Lijie Yang [a,b], Haiyan Wang [a,b], Xiaoyu Wei [a,b], Yanyan Shi [a,b], Dafeng Liang [c], Mingfeng Cao [a,b,**], Ning He [a,b,*]

[a] Department of Chemical and Biochemical Engineering, College of Chemistry and Chemical Engineering, Xiamen University, Xiamen, 361005, PR China
[b] The Key Lab for Synthetic Biotechnology of Xiamen City, Xiamen University, Xiamen, 361005, PR China
[c] Institute of Bioengineering, Guangdong Academy of Sciences, Guangzhou, 510316, Guangdong, PR China

ARTICLE INFO

Keywords:
Extracellular polymeric substance (EPS)
Polysaccharides
Transcriptome
Phosphate starvation

ABSTRACT

Extracellular polymeric substances (EPSs) are extracellular macromolecules in bacteria, which function in cell growth and show potential for mechanism study and biosynthesis application. However, the biosynthesis mechanism of EPS is still not clear. We herein chose *Bacillus licheniformis* CGMCC 2876 as a target strain to investigate the EPS biosynthesis. *epsK*, a member of *eps* cluster, the predicted polysaccharide synthesis cluster, was overexpressed and showed that the overexpression *of epsK* led to a 26.54% decrease in the production of EPS and resulted in slenderer cell shape. Transcriptome analysis combined with protein-protein interactions analysis and protein modeling revealed that *epsK* was likely responsible for the synthesis of teichuronic acid, a substitute cell wall component of teichoic acid when the strain was suffering phosphate limitation. Further cell cultivation showed that either phosphate limitation or the overexpression of teichuronic acid synthesis genes, *tuaB* and *tuaE* could similarly lead to EPS reduction. The enhanced production of teichuronic acid induced by *epsK* overexpression triggered the endogenous phosphate starvation, resulting in the decreased EPS synthesis and biomass, and the enhanced bacterial chemotaxis. This study presents an insight into the mechanism of EPS synthesis and offers the potential in controllable synthesis of target products.

1. Introduction

Bacterial extracellular polymeric substances (EPSs) have important applications for human beings. Due to their degradable, efficient, non-toxic and renewable properties, they are used in a wide range of applications in the pharmaceutical industry, the cosmetics industry, the food industry, agriculture and the bioremediation of pollution [1–3]. EPSs are composed of polysaccharides, proteins (e.g., γ-polyglutamic acid, γ-PGA), lipids, extracellular DNA, and humic substances, among which polysaccharides and proteins are the main components and the content can reach 75–90% [4,5]. Because of the complex composition and the many metabolic pathways involved, it is important to unravel the mechanisms of EPS synthesis for the exploitation and application of EPS.

We previously reported an *eps* cluster in the genome of *Bacillus licheniformis* CGMCC 2876, which was predicted to be responsible for the synthesis of exopolysaccharides [6]. In the cluster, several genes with demonstrated function have been identified, including encoding membrane sensors (*epsA*, *epsC*) [6–9], tyrosine protein kinases (*epsB*, *epsD*) [7–9], glycosyl modifying enzymes (*epsI*, *epsM*, *epsN*, *epsO*) [10–12], and a bifunctional glycosyltransferase (*epsE*) [13–15]. We characterized a gene designated *epsK*, which was annotated as an α-helical membrane transporter gene in *Bacillus subtilis* [16]. Other studies found that EpsK contains the conserved domain Wzx, and the protein was postulated to be a flippase or glycosyltransferase. EpsK is most likely responsible for

Abbreviations: EPS, Extracellular polymeric substance; γ-PGA, γ-polyglutamic acid; SEM, Scanning electron microscopy; DEGs, Differentially expressed genes; PPIs, Protein-protein interactions; QS, Quorum sensing.

☆ Grant numbers: National Natural Science Foundation of China (31871779, 32170061).Peer review under responsibility of KeAi Communications Co., Ltd.

* Corresponding author. Department of Chemical and Biochemical Engineering, College of Chemistry and Chemical Engineering, Xiamen University, Xiamen, 361005, PR China.

** Corresponding author. Department of Chemical and Biochemical Engineering, College of Chemistry and Chemical Engineering, Xiamen University, Xiamen, 361005, PR China.

E-mail addresses: mfcao@xmu.edu.cn (M. Cao), hening@xmu.edu.cn (N. He).

https://doi.org/10.1016/j.synbio.2022.04.001
Received 18 February 2022; Received in revised form 31 March 2022; Accepted 1 April 2022
Available online 5 April 2022

the transportation of polysaccharide repeating units from the cytoplasm to the periplasmic side [17,18]. Disruption of *epsK* led to an accumulation of poly-*N*-acetylglucosamine inside of *B. subtilis* cells [16]. During lipopolysaccharide synthesis, EpsK is responsible for the translation of the O-antigen, a repetitive glycan polymer which is subsequently added to rough lipopolysaccharide [19]. However, the function of *epsK* in *B. licheniformis* remains unclear.

In this study, we constructed an *epsK* overexpression strain of *B. licheniformis* and tried to shed light on the function of *epsK*, as well as the mechanism of EPS synthesis.

2. Materials and methods

2.1. Bacterial strains and growth conditions

B. licheniformis CGMCC 2876 was isolated by our laboratory [6]. *Escherichia coli* DH5α was grown in Luria–Bertani (LB) medium, which contained 1% tryptone, 0.5% yeast extract, and 1% NaCl, at 37 °C and 200 rpm. *B. licheniformis* was grown in LB or fermentation media at 37 °C and 200 rpm. Fermentation media refer to seed medium and EPS medium. LLP and LP medium provided phosphate starvation environment while HP150, HP200, HP250 and HP300 medium contained excess phosphate. Details of the medium composition were listed in Table S1.

For EPS production, *B. licheniformis* was primarily inoculated in seed medium and transferred to EPS medium as a 4% inoculum after 20 h.

2.2. Strain construction

Competent cell of *E. coli* was obtained from Ultra-Competent Cell Preps Kit (Sangon Biotech, Shanghai, China), while the competent cell of *B. licheniformis* CGMCC 2876 was prepared as reported [20]. Briefly, *B. licheniformis* was cultured in LB liquid medium containing 0.5 M sorbitol until mid-log phase, and the cells were collected at 4 ℃ and washed with pre-cooled electroporation medium (0.5 M sorbitol, 0.5 M mannitol and 10% glycerol) to prepare competent cells. The *epsK*, *tuaB*, *tuaE genes* were amplified using Phanta Master Mix (Vazyme, Nanjing, China), and the primers are listed in Table S2. Sequentially, the PCR products were cloned into the shuttle vector pHY300PLK-P*amyL*-TT*amyL*, a plasmid containing the promoter P*amyL* and terminator TT*amyL* constructed in our previous study [6], as KpnI/XhoI fragments and transformed into *E. coli* DH5α with selection on LB agar containing tetracycline (5 μg/ml). After verification, the correct plasmids were extracted from *E. coli* and transferred into *B. licheniformis* CGMCC 2876 by electroporation (25 kV/cm, 4 ms).

2.3. Purification of biopolymer and analysis of its composition

After the fermentation process, the biopolymer was extracted and purified using the method described in a previous study [21]. The content of total carbohydrates in the biopolymer was detected using the phenol–sulfuric acid method. Modified Bradford Protein Assay Kit (Sangon Biotech, Shanghai, China) was used to measure the protein content. The γ-PGA content was detected based on CTAB assay with incubation time adjusted to 10 min [22].

2.4. Analysis of biomass and bacterial morphology

To facilitate the determination of biomass, we measured the OD_{600} of the fermentation broth and subsequently collected the cells and lyophilised them for weighing, thus establishing a calibration curve relating biomass and optical density. The differences in morphology between the *epsK* overexpression strain OEK1 and wild-type strain 2876 were evaluated using SEM (S-4800, Hitachi, Tokyo, Japan) and the cells were collected after 24 h fermentation in EPS medium. The cells were washed with PBS (0.1 M, pH 7.2) three times before being fixed with 2.5% glutaraldehyde for 2 h. Additional washes were needed before hydrating the cells with 30, 50, 70, and 100% ethanol. The diameters of the bacteria were estimated using NanoMeasure software.

2.5. RNA-Seq

For RNA-seq, *B. licheniformis* CGMCC 2876 and OEK1 were primarily inoculated in seed medium and cultured for 20 h to the late logarithmic growth (OD~2), then transferred to EPS medium and further incubated for 24 h. The cells were collected by centrifugation at 8000 rpm for 10 min at 4 °C for total RNA purification and cDNA library construction. Sequencing was performed using the Illumina HiSeqTM 2500 platform with paired-end 150 base pair reads by Gene Denovo Biotechnology Co.

2.6. Analysis of transcriptome data

Raw data were filtered before the quality-trimmed reads were mapped to the genome of *B. licheniformis* CGMCC 2876 using Bowtie2 [23].The gene expression level was analyzed according to FPKM (fragments per kilobase of transcript per million). The edgeR package (http://www.r-project.org/) was used to identify DEGs with fold changes (FC)≥2 and FDR<0.05.

2.7. STRING

We chose the STRING database [24] to predict PPIs between EpsK and other proteins in *B. licheniformis*. In our analysis, we used neighborhood and co-occurrence checkboxes with a high confidence score of 0.7, while other checkboxes showed no results.

2.8. Modeling of EpsK

The modeling of EpsK was performed using I-TASSER (https://zhanglab.dcmb.med.umich.edu/I-TASSER/) and PyMOL (https://pymol.org/2/). The substrate and pathway informations were obtained from BioCyc (https://biocyc.org/). IonCom (https://zhanglab.dcmb.med.umich.edu/IonCom/) was used to predict the ion ligand binding site of EpsK.

2.9. Gene expression level analysis

As with RNA-seq samples, overexpression strains were also collected after 24 h of incubation for RNA extraction and gene expression analysis. Total RNA was extracted using a Bacterial RNA Kit (Omega Bio-Tek, Guangzhou, China) and quantified by a NanoDrop 2000 (Thermo, CA, USA). First-strand cDNA was synthesized using HiScript III RT SuperMix for qPCR (+gDNA wiper) (Vazyme, Nanjing, China), and qRT-PCR was performed with a qTOWER3 instrument (Analytik Jena AG, Jena, Germany) using ChamQ Universal SYBR qPCR Master Mix (Vazyme, Nanjing, China). The reference gene was 16S rRNA, and the relevant primers are listed in Table S2.

Availability of data and materials

The sequences data reported in this study have been deposited in the National Center for Biotechnology Information Sequence Read Archive (SRA), with the accession number PRJNA675185.

3. Results and discussion

3.1. The epsK functions in biopolymer synthesis of B. licheniformis

In our previous study, we found that *B. licheniformis* CGMCC 2876 could produce polysaccharides and γ-PGA under different culture conditions [21]. EpsK was reported to play an important role in polysaccharide biosynthesis, however, its exact function has not been characterized [16]. As shown in Table 1, the crude biopolymer

Table 1
Yields and compositions of biopolymers produced by *Bacillus licheniformis*.

		B. licheniformis CGMCC 2876	*B. licheniformis* OEK1
Production (g/L)		8.79 ± 0.26	6.56 ± 0.24
EPS Contents (%)	Protein	0.89 ± 0.05	0.49 ± 0.04
	Total sugar	3.48 ± 0.14	2.24 ± 0.09
	γ-PGA	20.74 ± 0.30	2.78 ± 0.08

production of the *epsK* overexpression strain *B. licheniformis* OEK1 was decreased by 26.54% compared to that of the wild-type *B. licheniformis* CGMCC 2876, indicating that *epsK* overexpression inhibits the production of biopolymers in *B. licheniformis*. Further analysis of the biopolymer contents showed an evident reduction in the proportions of γ-PGA, total sugar, and protein in OEK1, as the proportion of γ-PGA dropped from 20.74% to 2.78%. This implied that OEK1 synthesizes more undetectable components. We tentatively determined that EPS also contains undetectable components such as the applicable surfactants, but more detailed characterization will be performed in our future study.

3.2. The epsK functions in biomass and cell morphology

As shown in Fig. 1A, the *epsK* overexpression strain *B. licheniformis* OEK1 showed a 43.57% reduction in biomass compared to wild-type *B. licheniformis* CGMCC 2876 in the EPS medium at logarithmic phase and achieved a maximum at 20 h. In the mid-term period of fermentation, the biomass of the wild-type strain rapidly decreased. Meanwhile, the growth of OEK1 was relatively stable.

Scanning electron microscopy (SEM) was used to analyze the morphology of the cells collected at 24 h culture. The SEM micrographs showed that the morphology of the wild-type CGMCC 2876 tended to be short and thick, while the OEK1 cells were slender (Fig. 1D and E). It was calculated that the cell lengths of both strains were centralized at 2.5 μm, i.e., the cell length of the wild-type strain was ranging from 2.0 to 2.5 μm (33.33% of the total cell amount), while the length of OEK1 cells was mainly distributed between 2.5 and 3.0 μm (32.14% of the total cell amount) (Fig. 1B). In addition, there existed obvious difference in the cell width of the two strains. The cell width of 54.12% of the wild-type cells was distributed in the range of 0.5–0.7 μm, while the cell width of 77.01% of OEK1 cells was among 0.4–0.5 μm (Fig. 1C). It indicated that the *epsK* overexpression had effects on the cell propagation and cell morphology of *B. licheniformis*.

3.3. The epsK induces the global changes in the transcriptome

Principal component analysis (PCA) and Pearson correlation heat map analysis were performed to determine the correlation between the integrated data from the transcriptome data set (Figs. S1A and S1B). Quantitative real-time PCR (qRT-PCR) was performed to verify the credibility of transcriptome data (Figs. S1C and S1D). The results showed that the samples had high repeatability, and the data were suitable for subsequent analysis. We used the edgeR package to identify differentially expressed genes (DEGs) and obtained 1875 DEGs.

The analysis of GO (gene ontology) functional annotations revealed that DEGs were enriched for 29 functional terms. Among these terms, 14 terms were enriched in biological process, 8 terms in molecular function, and 7 terms in cellular component. Fig. 2A showed that 9 terms (single-organism process, response to stimulus, localization, locomotion, catalytic activity, transporter activity, membrane part, organelle part, and organelle) were significantly upregulated (≥60% genes). However, 7 terms (biological regulation, regulation of biological process, developmental process, transcription factor activity, protein binding, nucleic acid binding transcription factor activity, structural molecule activity, and macromolecular complex) exhibited obvious downregulation.

We collected the top 20 pathways with low Q value for significance analysis based on KEGG (Kyoto Encyclopedia of Genes and Genomes) (Fig. 2B) and obtained the four most significantly enriched pathways belonging to Metabolism, including starch and sucrose metabolism, the tricarboxylic acid cycle (TCA cycle), and carbon metabolism, which indicated an enhanced energy metabolism induced by *epsK* overexpression. There were also two enriched pathways belong to cellular processing, containing flagellar assembly and bacterial chemotaxis. Combined with the changes in the morphology of OEK1 cells, it suggested *epsK* overexpression not only led to a slenderer cell shape, but also resulted in an activated bacterial movement. In addition, aminoacyl-tRNA biosynthesis pathways were enriched as well, which may facilitate the protein synthesis of cells. We noted that some genes were also enriched and annotated to the pathway of photosynthesis and

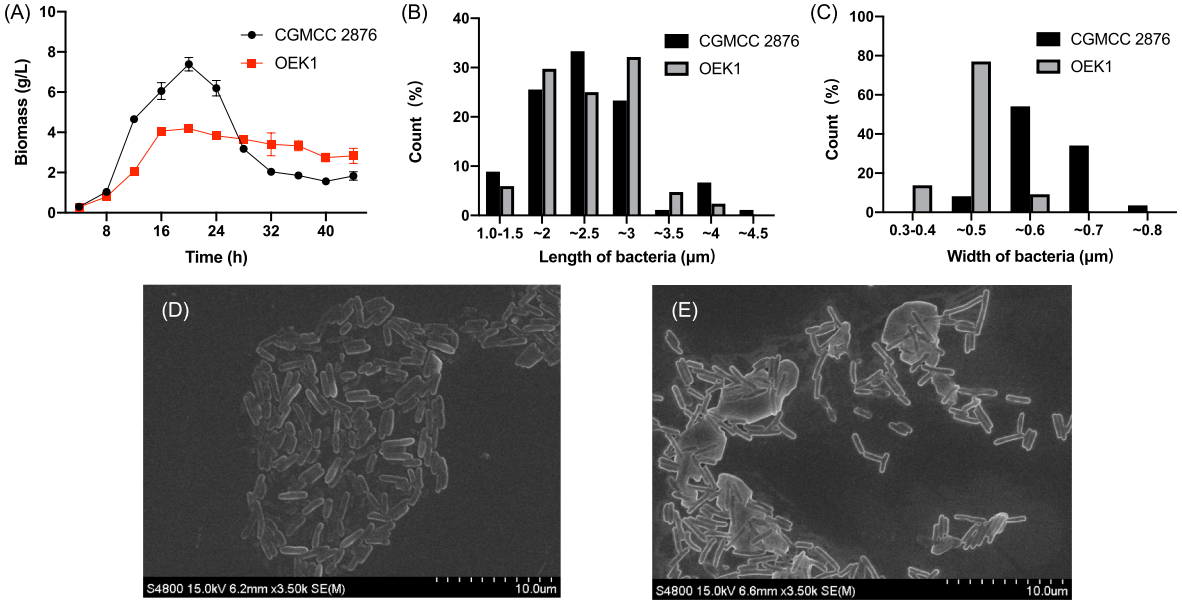

Fig. 1. Growth and morphology of *B. licheniformis*. (A) The growth curves of *B. licheniformis* strains in the EPS medium (mean ± standard error). (B) The statistics of bacterial length. (C) The statistics of bacterial width. (D) The SEM micrograph of *B. licheniformis* CGMCC 2876. (E) The SEM micrograph of *B. licheniformis* OEK1.

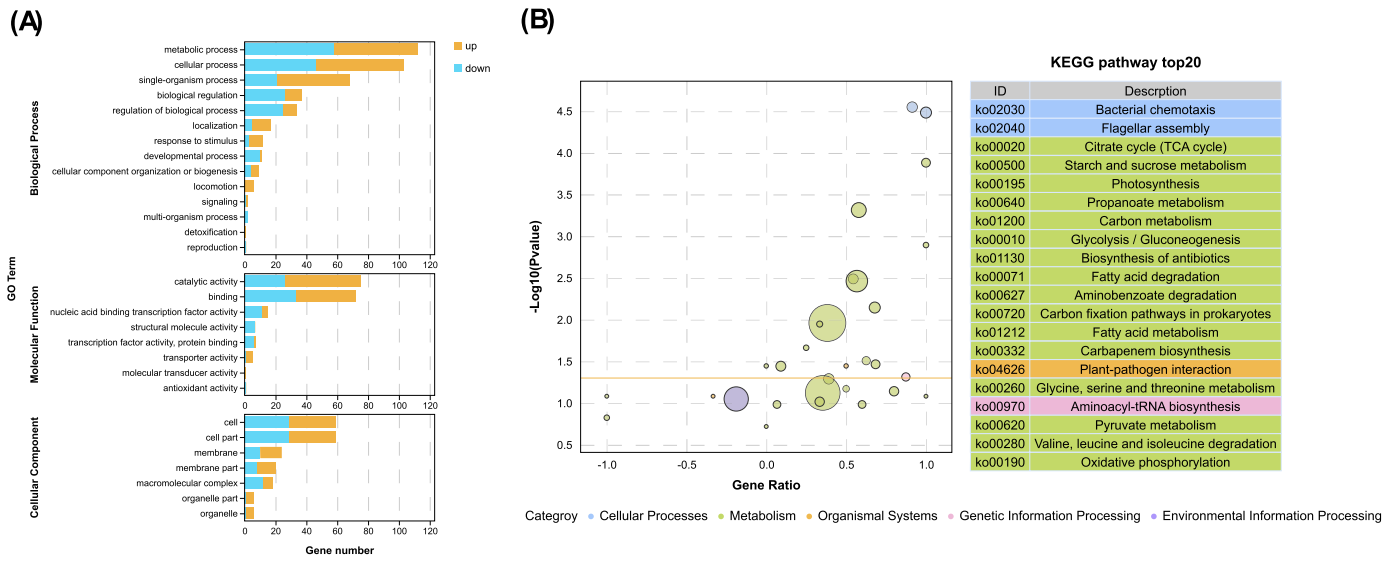

ID	Descrption
ko02030	Bacterial chemotaxis
ko02040	Flagellar assembly
ko00020	Citrate cycle (TCA cycle)
ko00500	Starch and sucrose metabolism
ko00195	Photosynthesis
ko00640	Propanoate metabolism
ko01200	Carbon metabolism
ko00010	Glycolysis / Gluconeogenesis
ko01130	Biosynthesis of antibiotics
ko00071	Fatty acid degradation
ko00627	Aminobenzoate degradation
ko00720	Carbon fixation pathways in prokaryotes
ko01212	Fatty acid metabolism
ko00332	Carbapenem biosynthesis
ko04626	Plant-pathogen interaction
ko00260	Glycine, serine and threonine metabolism
ko00970	Aminoacyl-tRNA biosynthesis
ko00620	Pyruvate metabolism
ko00280	Valine, leucine and isoleucine degradation
ko00190	Oxidative phosphorylation

Fig. 2. Functional enrichment of DEGs in *B. licheniformis* CGMCC 2876 vs OEK1. (A) The functional categories of DEGs based on GO. (B) The significance analysis of top 20 Q-value pathways based on KEGG.

plant-pathogen interaction, which does not imply that the bacterium is photosynthetic or a plant pathogen.

3.4. Functional speculation of epsK

To better understand the disturbance caused by *epsK* overexpression, the STRING database and Cytoscape were introduced to construct a network of protein-protein interactions (PPIs) between EpsK and other proteins (Fig. 3A and Table S3). It is noteworthy that 21 out of 42 genes were related to flagellar assembly, bacterial chemotaxis, and glycan metabolism, and most of these genes were upregulated. However, 21 genes associated with cell growth, transcription, transporters, and other pathways were downregulated. When combining PPIs and gene expression analyses, we noticed that the gene elements in the *eps* cluster, which interacted with *epsK*, only *epsC*, *epsG*, *epsL*, and *epsJ* showed detectable expression. This was associated with the decrease of polysaccharide content in the EPS.

It was interesting to observe that the trends in expression of *tuaE* and *tuaF* genes were consistent with *epsK*. As reported, the Wzy-type polymerase TuaE polymerizes repeating units in the periplasm [25]. TuaE is

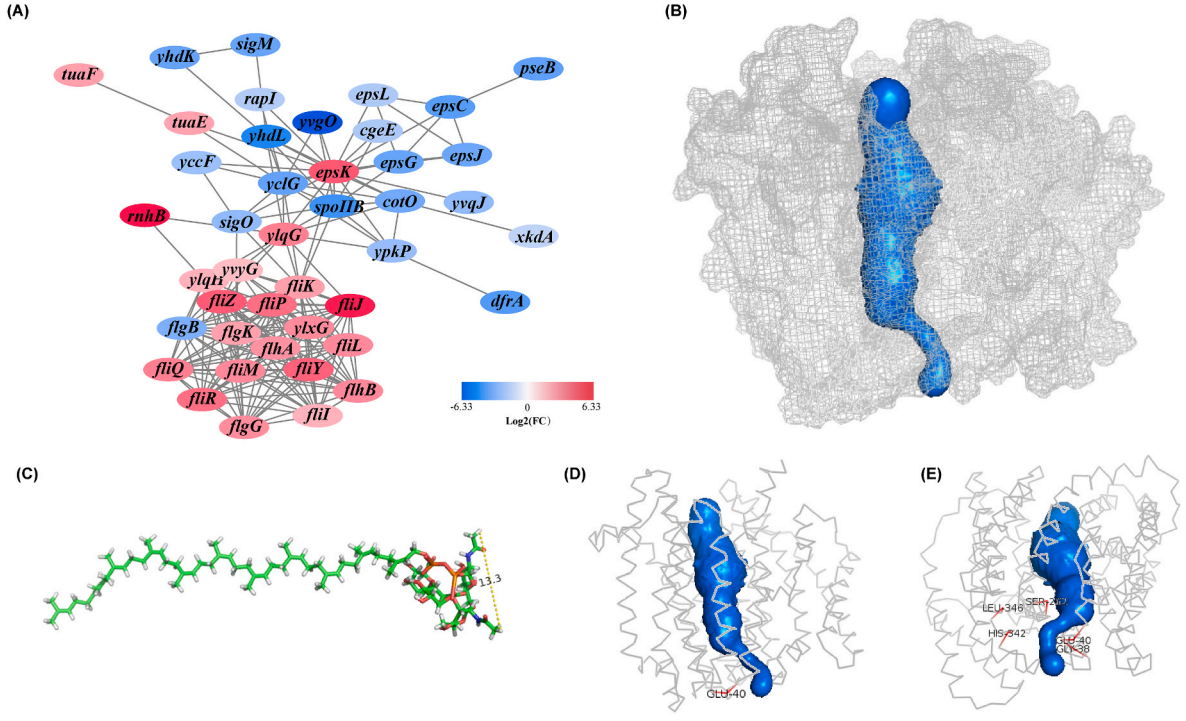

Fig. 3. Functional prediction of EpsK. (A) The differential expression levels of the genes included in the predicted PPIs of *epsK*. The network was constructed using Cytoscape. Each node represents a gene, and each line refers to an interaction. The circle colors revealed the expression level of the genes. (B) The protein model of EpsK (transport channel is marked in blue, while the protein is light gray). (C) The modeled sugar repeating unit. (D) Binding sites of EpsK and Zn^{2+}. Predicted binding residue: E40 (marked in red). (E) Binding sites of EpsK and Ca^{2+}. Predicted binding residues: G38, E40, S262, H342, L346 (marked in red). (For interpretation of the references to color in this figure legend, the reader is referred to the Web version of this article.)

functionally and structurally homologous to the PssT protein in *Rhizobium leguminosarum* bv. trifolii. Disruption of PssT in *R. leguminosarum* leads to an increase in the level of EPS production and the proportion of high-molecular-weight EPS [26]. TuaF contains a Wzz-domain, which acts as a co-polymerase that regulates the molecular weight of polysaccharides [27]. In *B. subtilis*, *tuaE* and *tuaF* belong to the operon required for the polymerization of teichuronic acid [28]. Teichuronic acid, like teichoic acid, is an important component of the cell wall. Under phosphate-limiting conditions, teichuronic acid is synthesized and replaces teichoic acid reduce the demand for phosphate [28–30].

Further analysis of gene expression in the teichuronic acid synthesis pathway revealed that *epsK* overexpression also led to the upregulation of *tuaD* and downregulation of *tuaB*. It was demonstrated that *tuaD* encoded UDP-glucose 6-dehydrogenase in *B. subtilis* 168, which converts UDP-glucose to UDP-glucuronate, and subsequently UDP-glucuronate was involved as a precursor substance in teichuronic acid synthesis [28]. The TuaB, on the other hand, was mainly responsible for the transmembrane transport of teichuronic acid repeating units [31]. Because TuaB shared the same Wzx structural domain as EpsK [17,18, 28], it was speculated that TuaB may compete with EpsK during the synthesis of teichuronic acid. Therefore, it exhibited an upregulation of *epsK* expression along with a downregulation of *tuaB* expression in the OEK1 strain. To summarize, we postulated that *epsK* is responsible for teichuronic acid synthesis and may be involved in the bacterial response to phosphate starvation.

In addition, the expression level of *ylqG* was upregulated due to the overexpression of *epsK*. However, *ylqG* has been rarely reported, except one reported that *ylqG* is part of the transcriptional organization of succinyl coenzyme A synthase (α subunit) [32]. *ylqG* may therefore be associated with the synthesis of succinyl coenzyme A synthase and the enhanced expression of *ylqG* may be responsible for the enhancement of TCA cycle in *B. licheniformis* OEK1.

We observed that *epsK* also interacted with 17 genes related to flagellar assembly and bacterial chemotaxis through *ylqG* and caused significant upregulation of 16 out of them [33–35].These 16 genes were *fliI-M*, *fliP-R*, *fliY-Z*, *yvyG*, *flnA-B*, *flgK*, *ylxG* and *flgG*. Bacterial chemotaxis, the targeted motions of cells following a gradient of chemo attractants, is often regarded as a bacterial starvation response induced upon nutrient depletion, or as a bacterial response to escape from a harmful environment [36]. It was speculated that there was an interconversion between the formation of biofilm and the maintenance of motility during bacterial growth, and that inhibition of bacterial motility would facilitate biofilm formation [37].

The modeling of EpsK was constructed to further elucidate its function (Fig. 3B). It was shown that there is a transmembrane transport channel in the EpsK protein (marked in blue), and the bottleneck of the channel is 3.006 Å. According to the pathway for the synthesis of teichuronic acid in *B. subtilis* 168 provided on BioCyc, the sugar repeat unit transported by flippase was β-D-glucuronosyl-(1 → 4)-β-D-glucuronosyl-(1 → 3)-*N*-acetyl-α-D-galactosaminyl-(1 → 6)-*N*-acetyl-α-D-galactosaminyl-diphospho-ditrans, octacis-undecaprenol (Fig. 3C). Since *B. licheniformis* is highly homologous to *B. subtilis*, they may share the same teichuronic acid repeat unit. The maximum width of the molecular model of the repeating unit, as measured by PyMOL, is about 13.3 Å, indicating that EpsK needs to change the configuration to achieve the transport of sugar repeating units.

It has been reported that when transporting the sugar repeating units, the Wzx domain contained in EpsK first binds to the cations from the periplasm to realize the configuration transformation and opens the transport channel toward the inside of the cell, and then binds to the sugar repeating units. Subsequently, the bound cations fall off, and the configuration of Wzx changes again toward the periplasm, thus realizing the reversal of sugar repeat units [27]. Using IonCom to predict the ion ligand binding site of EpsK, it was found that it may bind to Zn^{2+} at E40 (Fig. 3D) and Ca^{2+} at G38, E40, S262, H342, and L346 (Fig. 3E). This is consistent with the transport function of Wzx. Therefore, we speculated that EpsK was responsible for the export of teichuronic acid repeating units in *B. licheniformis* CGMCC 2876.

3.5. Putative mechanism of EPS synthesis

The above analysis indicated that the overexpression of *epsK* is correlated to teichuronic acid synthesis and phosphate starvation. As we know, starvation response is related to quorum sensing (QS), cell chemotaxis, Therefore, we selected the genes related to phosphate starvation response, QS, bacterial chemotaxis, and extracellular polymer synthesis for heatmap analysis. The possible metabolic and regulation mechanism of *epsK* in *B. licheniformis* CGMCC 2876 was constructed based on the heatmap analysis (Fig. 4).

Since teichuronic acid is an alternative to teichoic acid, teichoic acid synthesis pathway was analyzed and the expression of *tagA*, *tagB*, *tagD-F*, *tagG* and *tagO* were found to be decreased. It was reported that TagO, TagA, TagB, and TagD catalyzed the initial steps of teichoic acid synthesis to form lipid-anchored disaccharide glycerol 3-phosphate. TagE modified teichoic acid with α-glucose using UDP-glucose as a donor. TagF was responsible for adding 45–60 glycerol-3-phosphate units to the TagB product to form a polymer. TagG transported teichoic acid or teichoic acid precursor across the membrane [38,39]. Therefore, in *B. licheniformis* OEK1, teichuronic acid synthesis was enhanced accompanied with a weakened synthesis of teichoic acid.

The increase of teichuronic acid and the decrease of teichoic acid, which are the two important components of the cell wall of OEK1, may be the reason for the change of cell morphology. It was reported that the deletion of teichoic acid synthetase genes in *B. subtilis* inhibited teichoic acid production and changed the morphology of the mutants [40]. MreBH was demonstrated to be involved in the control of teichoic acid synthesis and the regulation of *lytE*. The *lytE* mutation of *B. subtillis* formed a longer cell chain and the cell diameter was smaller than that of the wild-type strain [41,42]. The change of cell wall compositions caused by the *epsK* overexpression resulted in the downregulation of *mreBH* and *lytE* in OEK1 strain, which made the cells slenderer than the wild-type strain.

As mentioned earlier, the overxpression of *epsK* enhanced teichuronic acid and inhibited teichoic acid synthesis, which was consistent with the physiological changes under phosphate starvation. We then analyzed the expression level of the key genes in bacterial phosphate starvation response, *phoP*, *phoR,* and *resABCDE*, which encode transcriptional activator PhoP, sensor kinase PhoR, and the two-component systems, respectively [43,44]. It was shown that these genes were upregulated in the strain of OEK1, which suggested the overexpression of *epsK* results in the phosphate starvation response. However, the alkaline phosphatase genes, *phoB* and *phoD*, which are responsible for harvesting phosphate from exogenous environment [43], were downregulated in OEK1. The results indicated that the response to phosphate starvation in OEK1 was caused by endogenous factors rather than exogenous factors, i.e., the strain generated phosphate starvation response in the absence of phosphate depletion.

QS system senses the signals from both the external environment and the cell itself, and then regulates the physiology changes of the cell, such as the EPS synthesis and the sporulation. QS is regulated by cell density: ComX is an extracellular cell density autoinducer, which is secreted to the periplasm by ComQ [45,46]. Periplasmic ComX binds to ComP and promotes the phosphorylation of ComP, ComA, DegQ and DegU sequentially, thereby enhance the synthesis of γ-PGA and surfactin and activate the phosphorylation of Spo0A [47,48]. Spo0A relieves the inhibition of SinR on *eps* gene cluster via increasing the expression of SinI, an anti-repressor of SinR, thus promoting the production of the extracellular matrix [49]. In *B. licheniformis* OEK1, *comQ*, *comA*, *degU,* and *spo0A* were downregulated compared to CGMCC 2876, resulted in the inhibitory effect of SinR on *eps* gene cluster. The gene expression analysis revealed that the CapBCA complex genes (*capA*, *capB*, and *capC*), which are responsible for the polymerization of γ-PGA [50], were

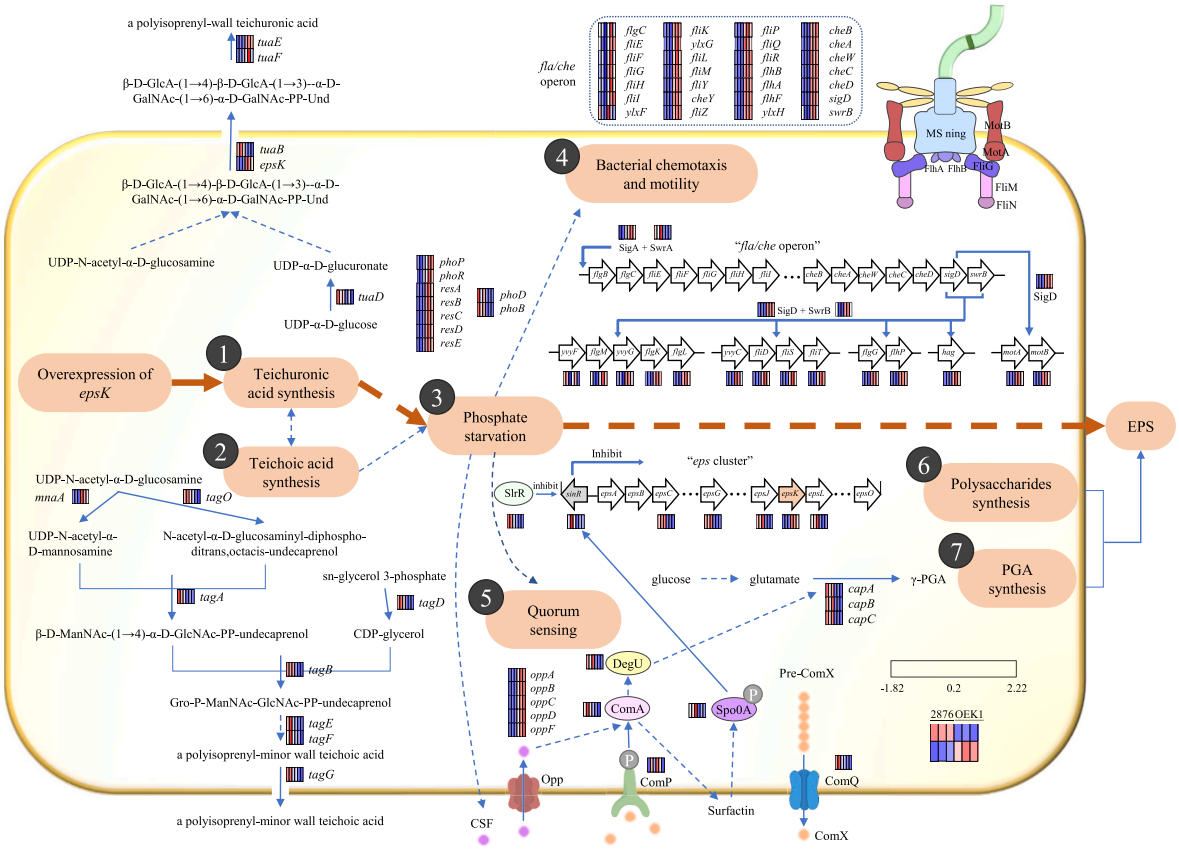

Fig. 4. The metabolic mechanism of EPS biosynthesis in *B. licheniformis*. The metabolic pathway was reconstructed based on BioCyc and KEGG analyses. Transcripts of *B. licheniformis* CGMCC 2876 and OEK1 are shown aside the pathway as a heat map based on fpkm in the transcriptome data. Note: (β-D-GlcA-(1 → 4)-β-D-GlcA-(1 → 3)-α-D-GalNAc-(1 → 6)-α-D-GalNAc-PP-Und represents β-D-glucuronosyl-(1 → 4)-β-D-glucuronosyl-(1 → 3)-*N*-acetyl-α-D-galactosaminyl-(1 → 6)-*N*-acetyl-α-D-galactosaminyl-diphospho-ditrans, octacis-undecaprenol).

downregulated, while the *eps* genes for polysaccharides synthesis were inhibited due to the suppression effect by SinR, leading a decrease of extracellular polymeric substances.

As we know, QS system is also regulated by CSF (competence and sporulation factor), which is induced by starvation and other external stimuli. Phosphorylation of ComA is inhibited by a certain concentration of intracellular CSF transported via oligopeptide permease Opp [45,46]. In the transcriptome of *B. licheniformis* OEK1, the oligopeptide permease gene *oppABCDE* was significantly upregulated, indicating that Opp may be transporting a large amount of CSF produced by phosphate starvation. It was reported that starvation signals bring the cell into a stable phase [46]. This may be the reason why *B. licheniformis* OEK1 entered the stable stage earlier and the biomass was lower than CGMCC 2876.

Additionally, the starvation response caused by nutrient consumption will enhance the chemotaxis of bacteria [36]. In *B. subtilis*, *fla/che* operon contains flagellum genes, chemotaxis genes, and regulatory genes *sigD* and *swrB*. SigD and SwrB are responsible for regulating the transcription of genes related to flagella synthesis outside the operon [51]. In strain of OEK1, the expression of *fla/che* operon and the genes regulated by *sigD* were significantly upregulated. The results indicated that *B. licheniformis* OEK1 exhibited an enhancement of bacterial chemotaxis under phosphate starvation response.

3.6. EPS production of *B. licheniformis* under phosphate starvation

Based on the previous speculations, we applied different concentrations of phosphate to *B. licheniformis* CGMCC 2876 for EPS production and further constructed *tuaB* and *tuaE* overexpression strains, *B. licheniformis* OETB and OETE, to investigate the relationship among techuronic acid synthesis, phosphate starvation, and EPS synthesis.

Like *B. licheniformis* OEK1, the overexpression of *tuaB* and *tuaE* induced the decrease in EPS production (Fig. 5A). When cultured in LLP medium, the crude biopolymer production of *B. licheniformis* CGMCC 2876 was 2.92 ± 0.43 g/L, a decrease of 66.09% compared to that of the strain cultured in EPS medium, which was 8.61 ± 0.51 g/L. The crude biopolymer production of *B. licheniformis* CGMCC 2876 increased with increasing phosphate concentration and reached a maximum at the highest phosphate concentration (HP300 medium) (Fig. 5B). The results indicated that phosphate starvation inhibited bacterial production of EPS.

Transcriptional analysis was performed using qRT-PCR to compare the related gene expression levels of *B. licheniformis* CGMCC 2876, OETB and OETE strains. As shown in Fig. 5C and D, the expression levels of phosphate starvation response genes were increased by 1.44~4.21-fold in *B. licheniformis* OETB, as well as teichuronic acid synthesis genes *tuaD* and *tuaE*. Differently, *epsK* was slightly downregulated (0.82-fold) due to the overexpression of *tuaB*, implying a possible functional competition between *epsK* and *tuaB*. In *B. licheniformis* OETE (Fig. 5E and F), the phosphate starvation response genes *phoP*, *resD* were moderately upregulated (1.45 and 1.21-fold respectively) while others were downregulated. The expression of *epsK* and *tuaB* were activated by the *tuaE* overexpression. When incubated at different phosphate concentrations, the expression of phosphate starvation response genes in *B. licheniformis* CGMCC 2876 showed a correlation with the changes in phosphate concentration, i.e., enhanced phosphate starvation response was exhibited at both low and high phosphate concentrations (Fig. 5G). Meanwhile, the expression of teichuronic acid synthesis genes showed a similar correlation (Fig. 5H), which indicated that teichuronic acid

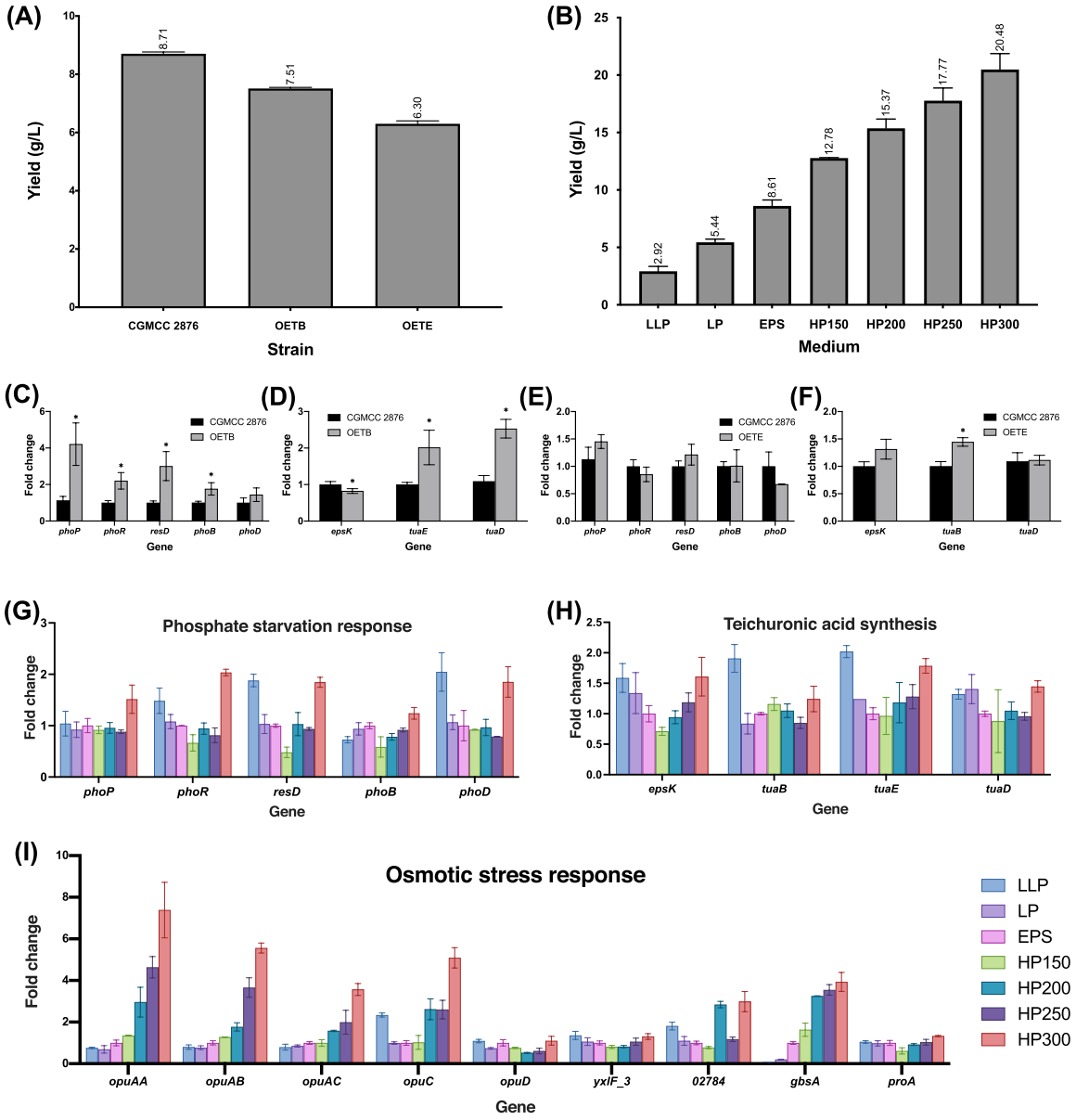

Fig. 5. The effect of phosphate starvation on the metabolism of *B. licheniformis*. (A) Crude biopolymer yield of *B. licheniformis* CGMCC 2876, OETB and OETE. (B) Crude biopolymer yield of *B. licheniformis* cultured under different concentrations of phosphate. (C) Analysis of gene expression in the phosphate starvation response pathway of *B. licheniformis* CGMCC 2876 and OETB. (D) Analysis of gene expression in the teichuronic acidsynthesis pathway of *B. licheniformis* CGMCC 2876 and OETB. (E) Analysis of gene expression in the phosphate starvation response pathway of *B. licheniformis* CGMCC 2876 and OETE. (F) Analysis of gene expression in the teichuronic acidsynthesis pathway of *B. licheniformis* CGMCC 2876 and OETE. (G) Analysis of gene expression in the phosphate starvation response pathway of *B. licheniformis* CGMCC 2876. (H) Analysis of gene expression in the teichuronic acid synthesis pathway of *B. licheniformis* CGMCC 2876. (I) Analysis of gene expression in the osmotic stress response pathway of *B. licheniformis* CGMCC 2876. Relative expression was determined by $2^{-\triangle\triangle Ct}$, $^{*}p < 0.05$ versus 2876.

synthesis and phosphate starvation response might also play a role in the osmotic stress response generated by high phosphate concentrations, and this hypothesis was confirmed by expression analysis of osmotic stress response genes [52] (Fig. 5I). Overall, we hypothesized that EpsK, like a flippase is involved in teichuronic acid synthesis and phosphate starvation response, and the overexpression of *epsK* had complex effects on cellular metabolism.

4. Conclusion

In summary, we found that overexpression of *epsK* in *B. licheniformis* CGMCC 2876 inhibited the synthesis of EPS and altered cell morphology and reproduction. Combining transcriptomics and PPIs analysis, we speculated that *epsK* is a flippase transporting teichuronic acid repeating units and the overexpression of *epsK* in *B. licheniformis* CGMCC 2876 stimulated endogenous phosphate starvation response, which then played roles in bacterial growth and morphology, EPS synthesis, bacterial chemotaxis, and QS. Further construction of *tuaB* and *tuaE* overexpression strains, as well as cell cultivation corroborated our suspicions above. Our results provided the putative functions of the *epsK* gene in *B. licheniformis*, which will benefit the researchers in manipulating the expression of stress response genes to make bacteria missense their metabolic states instead of imposing stress conditions, thereby regulating the synthesis of target products. This work also paves the way for further understanding the mechanism of EPS synthesis.

Funding

This work was financially supported by the National Natural Science Foundation of China (31871779 and 32170061).

CRediT authorship contribution statement

Yiyuan Xu: Conceptualization, Formal analysis, Investigation, Validation, Visualization, Writing – original draft, Writing – review & editing. **Lijie Yang:** Investigation, Validation. **Haiyan Wang:** Validation. **Xiaoyu Wei:** Investigation. **Yanyan Shi:** Visualization. **Dafeng Liang:** Writing – review & editing. **Mingfeng Cao:** Conceptualization, Project administration, Writing – review & editing. **Ning He:** Conceptualization, Funding acquisition, Project administration, Resources, Supervision, Writing – review & editing.

Declaration of competing interest

The authors declare that they have no competing interests.

Acknowledgements

We gratefully acknowledge SPRINGER NATURE Author Services (SNAS) for the editorial services.

Appendix A. Supplementary data

Supplementary data to this article can be found online at https://doi.org/10.1016/j.synbio.2022.04.001.

References

[1] Saha I, Datta S, Biswas D. Exploring the role of bacterial extracellular polymeric substances for sustainable development in agriculture. Curr Microbiol 2020;77 (11):3224–39. https://doi.org/10.1007/s00284-020-02169-y.
[2] Salehizadeh H, Yan N, Farnood R. Recent advances in polysaccharide bio-based flocculants. Biotechnol Adv 2018;36(1):92–119. https://doi.org/10.1016/j.biotechadv.2017.10.002.
[3] Freitas F, Alves VD, Reis MA. Advances in bacterial exopolysaccharides: from production to biotechnological applications. Trends Biotechnol 2011;29(8): 388–98. https://doi.org/10.1016/j.tibtech.2011.03.008.
[4] Sheng GP, Yu HQ, Li XY. Extracellular polymeric substances (EPS) of microbial aggregates in biological wastewater treatment systems: a review. Biotechnol Adv 2010;28(6):882–94. https://doi.org/10.1016/j.biotechadv.2010.08.001.
[5] More TT, Yadav JSS, Yan S, Tyagi RD, Surampalli RY. Extracellular polymeric substances of bacteria and their potential environmental applications. J Environ Manag 2014;144:1–25. https://doi.org/10.1016/j.jenvman.2014.05.010.
[6] Chen Z, Liu P, Li Z, Yu W, Wang Z, Yao H, et al. Identification of key genes involved in polysaccharide bioflocculant synthesis in *Bacillus licheniformis*. Biotechnol Bioeng 2017;114(3):645–55. https://doi.org/10.1002/bit.26189.
[7] Bridier A, Piard JC, Pandin C, Labarthe S, Dubois-Brissonnet F, Briandet R. Spatial organization plasticity as an adaptive driver of surface microbial communities. Front Microbiol 2017;8:1364. https://doi.org/10.3389/fmicb.2017.01364.
[8] Elsholz AK, Wacker SA, Losick R. Self-regulation of exopolysaccharide production in *Bacillus subtilis* by a tyrosine kinase. Genes Dev 2014;28(15):1710–20. https://doi.org/10.1101/gad.246397.114.
[9] Lekota KE, Bezuidt OKI, Mafofo J, Rees J, Muchadeyi FC, Madoroba E, et al. Whole genome sequencing and identification of *Bacillus endophyticus* and *B. anthracis* isolated from anthrax outbreaks in South Africa. BMC Microbiol 2018;18(1):67. https://doi.org/10.1186/s12866-018-1205-9.
[10] Lipa P, Vinardell JM, Kopcinska J, Zdybicka-Barabas A, Janczarek M. Mutation in the *pssz* gene negatively impacts exopolysaccharide synthesis, surface properties, and symbiosis of *Rhizobium leguminosarum* bv. Trifolii with clover. Genes (Basel) 2018;9(7). https://doi.org/10.3390/genes9070369.
[11] Kaundinya CR, Savithri HS, Rao KK, Balaji PV. EpsM from *Bacillus subtilis* 168 has UDP-2,4,6-trideoxy-2-acetamido-4-amino glucose acetyltransferase activity in vitro. Biochem Biophys Res Commun 2018;505(4):1057–62. https://doi.org/10.1016/j.bbrc.2018.09.185.
[12] Kaundinya CR, Savithri HS, Rao KK, Balaji PV. EpsN from *Bacillus subtilis* 168 has UDP-2,6-dideoxy 2-acetamido 4-keto glucose aminotransferase activity in vitro. Glycobiology 2018;28(10):802–12. https://doi.org/10.1093/glycob/cwy063.
[13] Guttenplan SB, Blair KM, Kearns DB. The EpsE flagellar clutch is bifunctional and synergizes with EPS biosynthesis to promote *Bacillus subtilis* biofilm formation. PLoS Genet 2010;6(12):e1001243. https://doi.org/10.1371/journal.pgen.1001243.
[14] Blair Kris M, Turner Linda, Winkelman Jared T, Berg Howard C, Kearns Daniel B. A molecular clutch disables flagella in the *Bacillus subtilis* biofilm. science 2008;320 (5883):1636–8.
[15] Kutschera A, Schombel U, Wrobel M, Gisch N, Ranf S. Loss of *wbpL* disrupts O-polysaccharide synthesis and impairs virulence of plant-associated *Pseudomonas* strains. Mol Plant Pathol 2019;20(11):1535–49. https://doi.org/10.1111/mpp.12864.
[16] Roux D, Cywes-Bentley C, Zhang YF, Pons S, Konkol M, Kearns DB, et al. Identification of poly-N-acetylglucosamine as a major polysaccharide component of the *Bacillus subtilis* biofilm matrix. J Biol Chem 2015;290(31):19261–72. https://doi.org/10.1074/jbc.m115.648709.
[17] Dong H, Zhang Z, Tang X, Paterson NG, Dong C. Structural and functional insights into the lipopolysaccharide ABC transporter LptB2FG. Nat Commun 2017;8(1): 222. https://doi.org/10.1038/s41467-017-00273-5.
[18] Wu S, Zheng R, Sha Z, Sun C. Genome sequence of *Pseudomonas stutzeri* 273 and identification of the exopolysaccharide EPS273 biosynthesis locus. Mar Drugs 2017;15(7). https://doi.org/10.3390/md15070218.
[19] Ruiz N, Kahne D, Silhavy TJ. Transport of lipopolysaccharide across the cell envelope: the long road of discovery. Nat Rev Microbiol 2009;7(9):677–83. https://doi.org/10.1038/nrmicro2184.
[20] Xue GP, Johnson JS, Dalrymple BP. High osmolarity improves the electro-transformation efficiency of the gram-positive bacteria *Bacillus subtilis* and *Bacillus licheniformis*. J.microbial.methods 1999;34(3):183–91. https://doi.org/10.1016/s0167-7012(98)00087-6.
[21] Liu P, Chen Z, Yang L, Li Q, He N. Increasing the bioflocculant production and identifying the effect of overexpressing *epsB* on the synthesis of polysaccharide and gamma-PGA in *Bacillus licheniformis*. Microb Cell Factories 2017;16(1):163. https://doi.org/10.1186/s12934-017-0775-9.
[22] Halmschlag B, Hoffmann K, Hanke R, Putri SP, Fukusaki E, Buchs J, et al. Comparison of isomerase and weimberg pathway for gamma-PGA production from xylose by engineered *Bacillus subtilis*. Front Bioeng Biotechnol 2019;7:476. https://doi.org/10.3389/fbioe.2019.00476.
[23] Langmead B, Salzberg SL. Fast gapped-read alignment with Bowtie 2. Nat Methods 2012;9(4):357–9. https://doi.org/10.1038/nmeth.1923.
[24] Szklarczyk D, Gable AL, Lyon D, Junge A, Wyder S, Huerta-Cepas J, Simonovic M, Doncheva NT, Morris JH, Bork P, Jensen LJ, Mering CV. STRING v11: protein-protein association networks with increased coverage, supporting functional discovery in genome-wide experimental datasets. Nucleic Acids Res 2019;47(D1): D607–13. https://doi.org/10.1093/nar/gky1131.
[25] Marczak M, Mazur A, Koper P, Zebracki K, Skorupska A. Synthesis of rhizobial exopolysaccharides and their importance for symbiosis with legume plants. Genes (Basel) 2017;8(12). https://doi.org/10.3390/genes8120360.
[26] Mazur A, Krol JE, Marczak M, Skorupska A. Membrane topology of PssT, the transmembrane protein component of the type I exopolysaccharide transport system in *Rhizobium leguminosarum* bv. trifolii strain TA1. J Bacteriol 2003;185(8): 2503–11. https://doi.org/10.1128/jb.185.8.2503-2511.2003.
[27] Islam ST, Lam JS. Wzx flippase-mediated membrane translocation of sugar polymer precursors in bacteria. Environ Microbiol 2013;15(4):1001–15. https://doi.org/10.1111/j.1462-2920.2012.02890.x.
[28] Soldo B, Lazarevic V, Pagni M, Karamata D. Teichuronic acid operon of *Bacillus subtilis* 168. Mol Microbiol 1999;31(3):795–805. https://doi.org/10.1046/j.1365-2958.1999.01218.x.
[29] Qi Y, Hulett FM. Role of Pho-P in transcriptional regulation of genes involved in cell wall anionic polymer biosynthesis in *Bacillus subtilis*. J Bacteriol 1998;180(15): 4007–10. https://doi.org/10.1128/JB.180.15.4007-4010.1998.
[30] Pragai Z, Harwood CR. Regulatory interactions between the Pho and sigma(B)-dependent general stress regulons of *Bacillus subtilis*. Microbiology 2002;148(Pt 5): 1593–602. https://doi.org/10.1099/00221287-148-5-1593.
[31] Lahooti M, Harwood CR. Transcriptional analysis of the *Bacillus subtilis* teichuronic acid operon. Microbiology (Read) 1999;145(Pt 12):3409–17. https://doi.org/10.1099/00221287-145-12-3409.
[32] Jurgen B, Tobisch S, Wumpelmann M, Gordes D, Koch A, Thurow K, et al. Global expression profiling of *Bacillus subtilis* cells during industrial-close fed-batch fermentations with different nitrogen sources. Biotechnol Bioeng 2005;92(3): 277–98. https://doi.org/10.1002/bit.20579.
[33] Khater L, Alegria MC, Borin PF, Santos TM, Docena C, Tasic L, et al. Identification of the flagellar chaperone FlgN in the phytopathogen *Xanthomonas axonopodis* pathovar citri by its interaction with hook-associated FlgK. Arch Microbiol 2007; 188(3):243–50. https://doi.org/10.1007/s00203-007-0240-y.
[34] Guttenplan SB, Shaw S, Kearns DB. The cell biology of peritrichous flagella in *Bacillus subtilis*. Mol Microbiol 2013;87(1):211–29. https://doi.org/10.1111/mmi.12103.
[35] Mukherjee S, Kearns DB. The structure and regulation of flagella in *Bacillus subtilis*. Annu Rev Genet 2014;48:319–40. https://doi.org/10.1146/annurev-genet-120213-092406.
[36] Cremer J, Honda T, Tang Y, Wong-Ng J, Vergassola M, Hwa T. Chemotaxis as a navigation strategy to boost range expansion. Nature 2019;575(7784):658–63. https://doi.org/10.1038/s41586-019-1733-y.
[37] Guttenplan SB, Kearns DB. Regulation of flagellar motility during biofilm formation. FEMS Microbiol Rev 2013;37(6):849–71. https://doi.org/10.1111/1574-6976.12018.
[38] Brown S, Santa Maria Jr JP, Walker S. Wall teichoic acids of gram-positive bacteria. Annu Rev Microbiol 2013;67:313–36. https://doi.org/10.1146/annurev-micro-092412-155620.
[39] Lazarevic V, Karamata D. The *tagGH* operon of *Bacillus subtilis* 168 encodes a two-component ABC transporter involved in the metabolism of two wall teichoic acids.

Mol Microbiol 1995;16(2):345–55. https://doi.org/10.1111/j.1365-2958.1995.tb02306.x.
[40] Bhavsar AP, Erdman LK, Schertzer JW, Brown ED. Teichoic acid is an essential polymer in *Bacillus subtilis* that is functionally distinct from teichuronic acid. J Bacteriol 2004;186(23):7865–73. https://doi.org/10.1128/JB.186.23.7865-7873.2004.
[41] Dominguez-Cuevas P, Porcelli I, Daniel RA, Errington J. Differentiated roles for MreB-actin isologues and autolytic enzymes in *Bacillus subtilis* morphogenesis. Mol Microbiol 2013;89(6):1084–98. https://doi.org/10.1111/mmi.12335.
[42] Kawai Y, Daniel RA, Errington J. Regulation of cell wall morphogenesis in *Bacillus subtilis* by recruitment of PBP1 to the MreB helix. Mol Microbiol 2009;71(5):1131–44. https://doi.org/10.1111/j.1365-2958.2009.06601.x.
[43] Hoi le T, Voigt B, Jurgen B, Ehrenreich A, Gottschalk G, Evers S, et al. The phosphate-starvation response of *Bacillus licheniformis*. Proteomics 2006;6(12):3582–601. https://doi.org/10.1002/pmic.200500842.
[44] Birkey SM, Liu W, Zhang X, Duggan MF, Hulett FM. Pho signal transduction network reveals direct transcriptional regulation of one two-component system by another two-component regulator: *Bacillus subtilis* PhoP directly regulates production of ResD. Mol Microbiol 1998;30(5):943–53. https://doi.org/10.1046/j.1365-2958.1998.01122.x.
[45] Bacon Schneider K, Palmer TM, Grossman AD. Characterization of comQ and comX, two genes required for production of ComX pheromone in *Bacillus subtilis*. J Bacteriol 2002;184(2):410–9. https://doi.org/10.1128/jb.184.2.410-419.2002.
[46] Lazazzera Beth A. Quorum sensing and starvation: signals for entry into stationary phase. Curr Opin Microbiol 2000;3(2):177–82. https://doi.org/10.1016/S1369-5274(00)00072-2.
[47] Kalamara M, Spacapan M, Mandic-Mulec I, Stanley-Wall NR. Social behaviours by *Bacillus subtilis*: quorum sensing, kin discrimination and beyond. Mol Microbiol 2018;110(6):863–78. https://doi.org/10.1111/mmi.14127.
[48] Stanley NR, Lazazzera BA. Defining the genetic differences between wild and domestic strains of *Bacillus subtilis* that affect poly-gamma-dl-glutamic acid production and biofilm formation. Mol Microbiol 2005;57(4):1143–58. https://doi.org/10.1111/j.1365-2958.2005.04746.x.
[49] Chai Y, Norman T, Kolter R, Losick R. An epigenetic switch governing daughter cell separation in *Bacillus subtilis*. Genes Dev 2010;24(8):754–65. https://doi.org/10.1101/gad.1915010.
[50] Cao M, Feng J, Sirisansaneeyakul S, Song C, Chisti Y. Genetic and metabolic engineering for microbial production of poly-gamma-glutamic acid. Biotechnol Adv 2018;36(5):1424–33. https://doi.org/10.1016/j.biotechadv.2018.05.006.
[51] Kearns DB, Losick R. Cell population heterogeneity during growth of *Bacillus subtilis*. Genes Dev 2005;19(24):3083–94. https://doi.org/10.1101/gad.1373905.
[52] Schroeter R, Hoffmann T, Voigt B, Meyer H, Bleisteiner M, Muntel J, et al. Stress responses of the industrial workhorse *Bacillus licheniformis* to osmotic challenges. PLoS One 2013;8(11):e80956. https://doi.org/10.1371/journal.pone.0080956.